CIRP Annals - Manufacturing Technology 73 (2024) 117–120

Contents lists available at ScienceDirect

CIRP Annals - Manufacturing Technology

journal homepage: https://www.editorialmanager.com/CIRP/default.aspx

Submerged electrochemical jet machining with in-situ gas assistance

Yonghua Zhao[a,*], Zhaozhi Lyu[a], Weidong Liu[b], Bi Zhang (1)[a], Adam T. Clare (1)[c]

[a] Department of Mechanical and Energy Engineering, Southern University of Science and Technology, Shenzhen 518055, China
[b] College of Aeronautical Engineering, Civil Aviation University of China, Tianjin, 300300, China
[c] Department of Mechanical Engineering, The University of British Columbia, Vancouver, V6T 1Z4, Canada

ARTICLE INFO

Article history:
Available online 1 May 2024

Keywords:
Electro chemical machining
Electrolyte jet

ABSTRACT

Electrochemical jet machining (EJM) on concave surfaces or cavities is challenging because the jet and film flow fail to form. This work presents an in-situ electrolytic gas and plasma assistance approach to enable EJM under electrolyte. A structured nozzle cathode induces pressurized and insulating gas around electrolyte at the gap, generating a constrained jet and film flow. This serves to allow a precise and effective submerged EJM (SEJM) routine. Compared to EJM in air, SEJM shows more concentrated current distribution owing to a thinner film flow by the gas assistance, leading to a 65 % improvement in surface finish and a 16 % reduction of machining overcut.

1. Introduction

Electrochemical jet machining (EJM) enables the efficient machining of surface microfeatures in tough metals while providing mechanical and thermal stress-free high surface integrity [1–3]. Compared to other electrochemical machining methods, EJM is advantageous in obtaining localized high current density and high flow field by using a fine electrolyte jet as the cathode tool, leading to excellent dissolution performance.

However, when EJM is applied to large concave surfaces or deep small cavities, the electrolyte is difficult to drain and easily stays in the working area, eventually submerging the nozzle. Under electrolyte submersion, the electrolyte jet and surrounding thin film flow definitive for EJM cannot be formed, causing the current density distribution to spread. As a result, EJM fails to perform selective and localized micromachining.

Applying an assistive gas is one prominent approach to generating thin film flow in EJM. An additional jet of compressed air removes the electrolyte enclosing nozzle caused by surface tension, enabling a reduced working gap EJM [4]. The shear force of the coaxial gas flow discharges the electrolyte from accumulating in the machining area, achieving concaving surface machining even at low flow rates [5]. Further, the coaxial two-phase flow enables control over jet diameter via flow focus principle [6]. Applying air assistance in jet electrodeposition also shows a higher deposition rate and accuracy [7]. Meanwhile, these approaches may increase the complexity of EJM equipment. It is challenging to apply auxiliary airflow equipment when the workspace is small. On the other hand, electrolytic gas or plasma built around a tool electrode has been applied as an assistive technique in gas-enhanced electrochemical micromachining [8] and spark-assisted chemical etching [9,10]. In the present work, we propose inducing cathodic gas as in-situ assistance to achieve submerged EJM (SEJM) by innovating the process design. Previous studies have demonstrated hydrogen gas/plasma formation at the nozzle cathode in EJM under extreme current densities [11]. The study utilizes the cathodic gas and plasma phenomena to generate a constrained jet and film flow under electrolyte, achieving SEJM without adding extra apparatus to the traditional EJM and showing potential for flow focusing.

2. Principle of in-situ gas-assisted SEJM

Submerged EJM is realized using a surface-insulated metallic nozzle closely placed to the workpiece while applying a pulse voltage to the gap (Fig. 1a). The electrolyte is circulated through the nozzle. The nozzle's outer surface is mostly insulated to eliminate stray current, while a small portion of the nozzle tip is exposed to electrolyte to serve as the cathode. The cathode induces hydrogen gas evolution

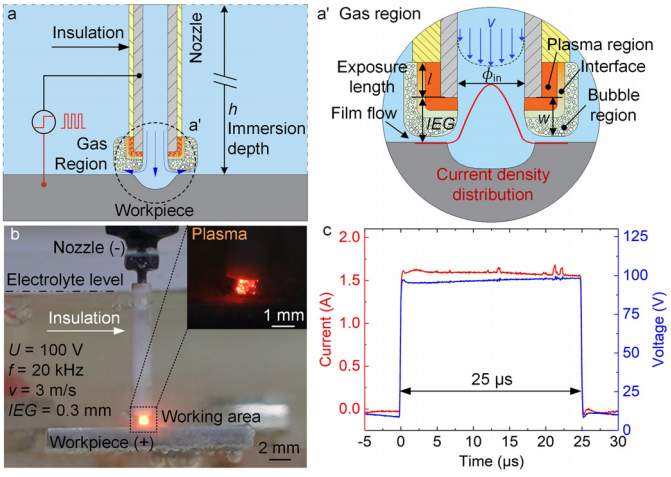

Fig. 1. (a) The principle of in-situ gas-assisted SEJM. (b) Photo of SEJM process in the presence of cathodic plasma. (c) Typical electrical waveform. The gas assistance allows enhanced process capability through greater surface finish and reduced overcut.

* Corresponding author.
E-mail address: zhaoyh@sustech.edu.cn (Y. Zhao).

https://doi.org/10.1016/j.cirp.2024.04.051
0007-8506/

upon applying potentials, which evolves into electrolytic plasma by cathodic discharges [12,13]. Thus, a partially ionized and pressurized gas region (GR) develops at the nozzle tip, constraining the local electrolyte flow. Matching the interelectrode gap (IEG) size with the GR enables the formation of a jet and film flow at the gap, concentrating the current density distribution. Further, the gas region exhibits great electrical resistance owing to its dominant gaseous property [14], shielding stray currents through the nozzle surfaces. As a result, a near-EJM condition is achieved under electrolyte, and the material is selectively removed under the jet, just like conventional EJM.

Further, compared to EJM in air, the kinetic and pressurized gas evolution at the gap in SEJM promotes a thinner film flow, potentially leading to improved machining performances. Through a fundamental understanding of process physics, a full description of the process behavior can be obtained.

3. Material and methods

The apparatus for investigating SEJM consisted of an electrolyte flushing system and a motion stage, allowing for nozzle positioning. A high-frequency power amplifier controlled by a function generator was employed as the electrical supply. Constant voltage control was used in experiments to induce gas while avoiding abnormal discharges. The applied pulse voltage (U) had a square waveform with adjustable frequency (f), allowing the control of gas region stability. For simplicity, the duty factor was kept at 50 % for all experiments. A stainless-steel nozzle of 600 μm inner diameter (Φ_{in}) was negatively biased to work as the cathode. Except for the tip, the nozzle's outer surface was insulated using a 0.5 mm thick heat-resistant ceramic; all machining experiments were undertaken on the SUS304 stainless steel workpiece in 20 wt.% $NaNO_3$ electrolyte, and the immersion depth (h) was set at 10 mm. The electrical signals during machining were collected using a voltage (TPP0500B, Tektronix) and current probe (TCP0030A, Tektronix). The resulting surfaces and geometries were characterized by a scanning electron microscope (SEM, Zeiss Merlin) and a contact stylus instrument (Surfcom NEX 031, Accretech).

4. Results and discussion

4.1. Validation of gas evolution and its effect on SEJM

The availability of a stable gas region is the key consideration in achieving SEJM. To validate this, SEJM drilling was carried out under various conditions using a nozzle exposure length of 1 mm. From experimental results, increasing the voltage promotes more gas evolution by electrolysis. Beyond a critical potential, typically > 100 V for the arrangement used here, the Faraday electrolysis regime at the cathode is superseded by a discharge-driven mechanism. The high potentials cause excessive insulating gas evolution at the gap, inducing cathodic discharges, as observed in Fig.1b. The discharge occurs at the cathode, accompanied by visible emission, which illuminates the gas region orange. Fig.1c shows a typical current waveform of the process, which exhibits minor oscillation due to discharge events. Meanwhile, the current slightly drops with pulse duration, implying increased gap resistance due to gas accumulation.

To examine the effect of gas assistance on the machining performance, SEJM drilling experiments were carried out at 100 V. The electrode size, i.e., the nozzle exposure length (NEL), was varied to regulate gas evolution. Fig. 2a shows that the machining overcut (relative to the nozzle inner diameter) initially decreased and then increased with increasing the NEL, implying a changing gas state at the machining gap. Notably, with increasing the exposure from 0 to 1 mm, the measured current decreased by 16 %, and the machining overcut reduced by 33.3 %, implying enhanced gas formation with increasing the electrode size. However, excessive exposure length, > 2 mm for this case, resulted in significantly increased overcut. This can be attributed to the enlarged exposed area reducing the current density at the cathode, leading to a reduced gas insulation effect and increased stray current. This is also verified by the drastic increase of machining current with increasing the NEL to 2 mm (Fig. 2b).

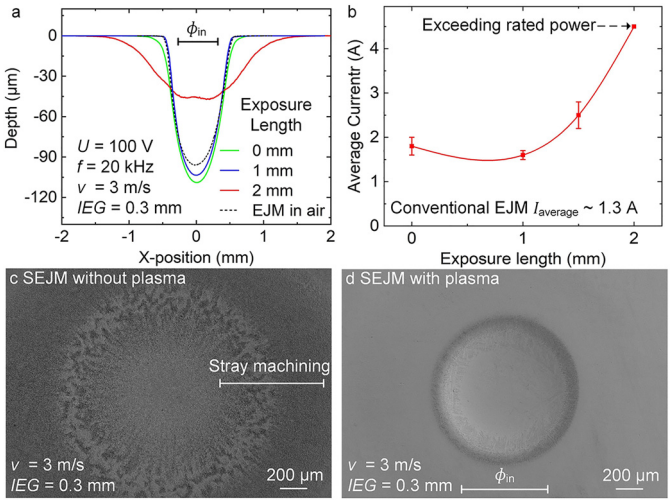

Fig. 2. Validation of gas assistance in SEJM drilling with a pulse frequency of 20 kHz for 5 s. (a) SEJM-resulted profiles with different nozzle exposure lengths. (b) Measured current during machining. (c) Typical pit machined at 60 V without plasma. (d) Typical pit machined at 100 V with plasma formation. Varying voltages and electrode sizes allow both ECM 'field' and electrolytic plasma formation to be explored.

Notably, compared to no exposure, an appropriate NEL resulted in the smallest overcut competitive with that of EJM in air owing to the enhanced gas assistance. These results show the effectiveness of gas assistance in improving the machining precision and its dependency on electrode size. To ensure precision SEJM, the following study used a 1 mm nozzle exposure length.

4.2. Cathodic contact glow discharge plasma

From Fig. 1, the assistive role of gas in realizing SEJM is reflected in two aspects: 1) generating the jet and film flow and 2) shielding stray current. A high-quality gas region is indispensable to achieving high-precision SEJM. Specifically, the size and pressure of the gas region should match with the IEG and electrolyte flow, respectively, to create a constrained laminar jet at the gap. Meanwhile, the gas region should be continuous and compact to isolate stray currents at the nozzle tip effectively. SEJM drilling experiments show that more localized removal and smoother surface can be obtained when cathodic contact glow discharge plasma (CGDP) [14] appears in the gas region, compared to pure gas assistance without plasma, see Fig. 2cd. The developed CGDP is surrounded by a bubble region isolating the working electrode surface from the electrolyte, enhancing the insulation effect. Moreover, the discharge potentially induces local pressure, providing a mechanical impulse to the surrounding electrolyte. This is beneficial for thinning the film flow, thus improving SEJM performance. The cathodic discharge may be regulated through electrical settings, but the IEG condition will also affect this. Excessive high potential or small IEG should be avoided to eliminate abnormal arcing.

4.3. Influences of the applied electrical conditions

In performing SEJM milling, it is crucial to maintain the stability and consistency of the gas region to ensure precision in machining. To realize stable gas and plasma formation at the machining gap, the influence of pulse frequency on SEJM milling was investigated. The machining voltage was 100 V. Since observing the gas distribution directly is difficult, the current signals during machining were studied to identify gas states. As shown in Fig. 3ab, a low pulse frequency causes high average current and violent current oscillation, implying instability of the gas region. This may be attributed to bubble dissipation and gas film breakage caused by long pulse intervals. In comparison, a high pulse frequency, 30 kHz for this case, significantly improves the process stability, evidenced by the stable and consistent current values (Fig. 3b). It is considered that a high pulse frequency effectively mitigates violent gas evolution and reduces individual discharge energy, beneficial for the stabilization of gas region [11].

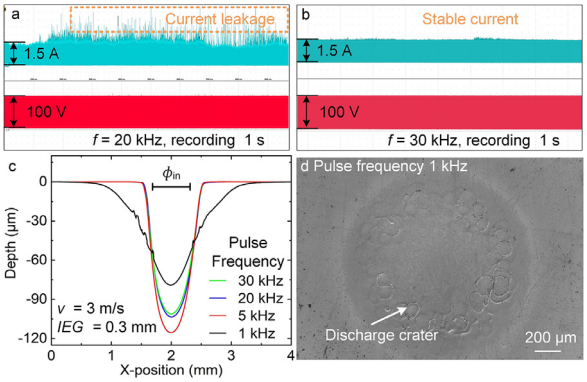

Fig. 3. Influence of pulse frequency on SEJM process. (a-b) Voltage and current signals during SEJM milling. (c) Variation of SEJM drilled profiles with changing the pulse frequency. (d) Abnormal discharges occur at 1 kHz.

Fig. 3cd shows the experimental results of SEJM drilling at 100 V. Increasing the pulse frequency from 1 kHz to 30 kHz leads to an evident reduction of the machining overcut, verifying the improvement of gas region stability discussed above. Notably, low frequencies of 1 kHz or less cause significant process instability, manifested as the occurrence of violent spark discharge and formation of discharge crater on the machined surface (Fig. 3d). The violent discharge can be ascribed to the long duration and excessive energy of a single pulse applied to the machining gap. This phenomenon is undesirable as it can cause considerable electrode wear and machined surface damage. For this reason, a high frequency is applied in SEJM. Meanwhile, in the high-frequency region > 5 kHz, the machining depth slightly decreased with increasing the pulse frequency, indicating reduced current efficiency with frequency rise.

4.4. Electrolyte flow velocity

The electrolyte flow velocity (v) plays a key role in process behavior by affecting the gas region behavior and electrolyte renewal. To experimentally validate this, SEJM drilling experiments with varying flow velocities were conducted. As shown in Fig. 4a, with increasing the flow velocity, the machined profiles get deeper while the machining overcut slightly increases. Excessive flow velocities (> 5 m/s for this case) lead to significantly enlarged overcut, indicating that the gas region fails to form at high flow velocities due to the excessive momentum of the electrolyte flow pushing the plasma and gas out. As a result, the electric field cannot be locally constrained at the machining gap, increasing the stray current effect.

On the other hand, despite the smaller overcut at 0.5 m/s, repeated experiments showed that the resulted pits tended to exhibit irregular shapes and uneven material removal, suggesting a distorted electric field distribution at low flow velocities. Also, the machining depth reduced. These are attributed to overloaded electrolytic products in the machining area, which caused uneven and lowered electrical conductivity at the working gap, as illustrated in Fig. 4c (left). These experimental results demonstrate that a moderate electrolyte flow velocity is required for SEJM to stabilize the gas region in the periphery of the constrained jet and ensure efficient dissolution in the machining spot.

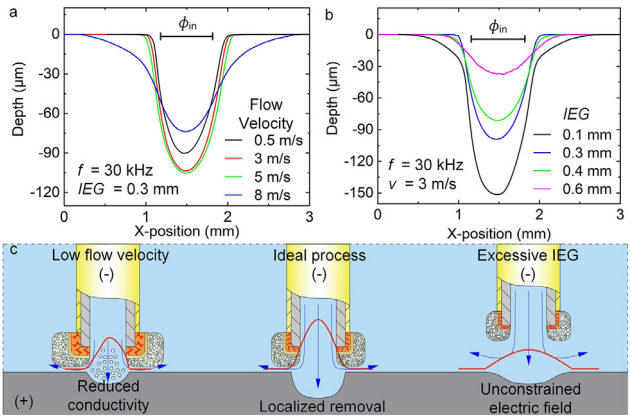

Fig. 4. Change of SEJM drilled profiles with a variation of (a) flow velocity and (b) interelectrode gap. (c) Illustration of process mechanisms under various conditions.

4.5. Interelectrode gap distance (IEG)

As illustrated in Fig. 1, the size of the gas region should match with the IEG to effectively create a jet and film flow. Fig. 4b shows the significance of IEG on SEJM drilling performance. The machined geometry improves drastically by reducing the IEG because of a more concentrated current density distribution at smaller gaps (Fig. 4c, middle). Specifically, the machining depth improved by 66.7 %, and the overcut decreased by 125 % when the IEG reduced from 0.6 mm to 0.3 mm. However, further IEG reduction to 0.1 mm caused a drastic increase of the overcut by 600 μm, indicating the failure of the gas region in constraining the electric field. This can be ascribed to violent gas evolution and discharges caused by an excessively increased electric field at the reduced gap, destabilizing the gas region [11]. Moreover, when the IEG is too small, the electric field strength likely surpasses the threshold to induce interelectrode spark discharge, which should be avoided as its high tensity damages the nozzle.

The mechanism by which the IEG affects the process is depicted in Fig. 4c. A large IEG makes it difficult to create the constrained jet and film flow because the size of the gas region is too small compared to the gap distance (Fig. 4c, right), resulting in unlocalized electric field and consequently unlocalized material removal. At a moderate IEG (0.3 mm for this case, Fig. 4c middle), the pressurized gas region occupies most of the gap, facilitating a constrained jet and film flow. Thus, the current flow is constrained in the machining gap, resulting in highly localized material removal. Hence, an appropriate IEG is essential in SEJM.

4.6. Parameter design for optimal process control

The above study has demonstrated three key process parameters in SEJM: 1) applied voltage and its frequency, 2) electrolyte flow velocity, and 3) interelectrode gap, which allows for precise design of the SEJM process. Meanwhile, the matching design of these parameters is of significance to SEJM precision due to their strong interactions. The optimal parameter combination provides a stable gas region of size and pressure comparable to that of the IEG and electrolyte flow, respectively. Through this, the flow and electric field can be restricted to a limited area, creating a local near-EJM environment.

Here, machining overcut is employed as a key index to assess SEJM precision. The general overcut of conventional EJM in air is about 0.3–0.6 times the nozzle's inner diameter. Therefore, the SEJM is inferior if the machining overcut exceeds half of the nozzle's inner diameter. Based on this criterion, the process window was experimentally investigated using SEJM drilling experiments, considering the matching of key process parameters. From the experimental results in Fig. 5, the voltage should be within an appropriate range to ensure a stable plasma generation and gas region formation. Meanwhile, the voltage should be limited to avoid violent gas evolution or arcing, which develops turbulence and considerably destabilizes gas

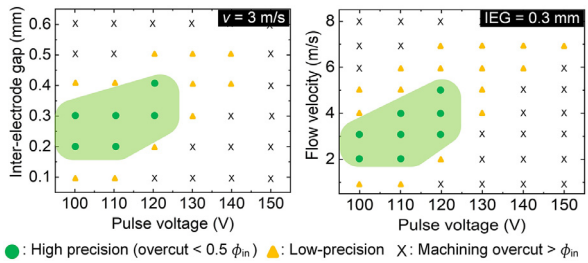

Fig. 5. Influence of key parameters and their interactions on SEJM precision. Investigation of IEG and flow velocity reveals a serviceable process window for this technique.

region formation, making it difficult to achieve precision SEJM. Furthermore, when the applied voltage increases, the IEG and electrolyte flow velocity should be adjusted accordingly. The adjustments are essential to assure the formation of a stable gas region while avoiding insufficient electrolyte supply and excessive electric field strength at the machining gap. Within the optimal process window, the green area in Fig. 5, stable, and precision SEJM were successfully carried out, showing a maximum overcut $< 0.5\ \Phi_{in}$.

4.7. Improved performance as compared to EJM in air

To examine the difference in machining performances, a comparative study of surface grooving between SEJM under electrolyte and conventional EJM in air was conducted (Fig. 6), with the machining conditions kept the same.

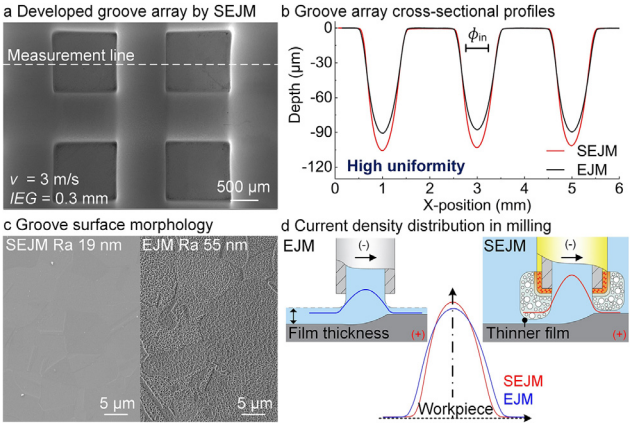

Fig. 6. (a) Groove array by SEJM. (b) Comparison of groove profiles and (c) resulted surfaces between SEJM and EJM. (d) Comparative illustration of current density distribution between EJM and SEJM milling. Through consideration of the process window, it is possible to arrive at metallurgically perfect surfaces, demonstrating the value of the SEJM process. (Voltage 100 V, 30 kHz, nozzle traverse speed 10 mm/s, milling passes 30).

Fig. 6a shows the machined grooves by in-situ gas-assisted SEJM, which exhibit a consistent, sharp profile with a smooth surface, demonstrating the process stability of SEJM. The comparison of groove cross-sectional profiles in Fig. 6b shows that the average groove depth by SEJM is 1.13 times that of EJM in air, while the overcut reduces by 16 % with SEJM. Moreover, compared to EJM in air, SEJM exhibits considerably improved surface integrity (Fig. 6c). The groove surface roughness by SEJM measures only Ra 19 nm compared to Ra 55 nm by EJM in air. Further, the pitting phenomena observed in EJM cannot be found in SEJM-resulted surface, indicating that SEJM provided a more concentrated current density distribution as compared to EJM in air, see Fig. 6d. The reason is considered that the in-situ gas and plasma assistance promote thinning the film flow by its hydrodynamic action, reducing the low current density region. These results demonstrated the process strength of SEJM over EJM in air.

5. Conclusions

Submerged EJM is realized by utilizing a novel electrolytic gas/plasma effect on electric field confinement to create a "near-EJM" environment under electrolytes. The stable insulation of the local gas region around the gap, manifested as cathodic discharge occurrence, ensures high-uniformity micromachining. The pressure and dynamics of gas evolution promote a thinner radial film flow of the impinging jet, reducing the low current density region. As a result, submerged EJM improves machining overcut and surface integrity as compared to those by EJM in air. The in-situ gas assistance approach enables EJM in large concave surfaces or deep cavities without additional equipment, further enhancing the process flexibility.

Declaration of competing interest

The authors declare that they have no known competing financial interests or personal relationships that could have appeared to influence the work reported in this paper.

CRediT authorship contribution statement

Yonghua Zhao: Conceptualization, Funding acquisition, Methodology, Project administration, Resources, Supervision, Writing – review & editing. **Zhaozhi Lyu:** Data curation, Investigation, Validation, Visualization, Writing – original draft. **Weidong Liu:** Formal analysis, Methodology. **Bi Zhang:** Formal analysis, Methodology, Resources. **Adam T. Clare:** Formal analysis, Methodology, Writing – review & editing.

Acknowledgments

This work was supported by the National Key Research and Development Program of China (2021YFF0501700), Guangdong R&D Program (2023ZDZX2023), and Shenzhen R&D Program (20231120141540001).

References

[1] Ippolito R, Tornincasa S, Capello G, Micheletti GF (1981) Electron-Jet Drilling - Basic Involved Phenomena. *CIRP Annals* 30(1):87–90.
[2] Kunieda M, Yoshida M, Yoshida H, Akamatsu Y (1993) Influence of Micro Indents Formed by Electro-chemical Jet Machining on Rolling Bearing Fatigue Life. *ASME PED* 64:693–699.
[3] Speidel A, Bisterov I, Saxena KK, Zubaye M, Reynaerts D, Natsu W, Clare AT (2022) Electrochemical Jet Manufacturing Technology: From Fundamentals to Application. *International Journal of Machine Tools and Manufacture* 180:103931.
[4] Hackert M, Meichsner G, Schubert A (2008) Generating Micro Geometries with Air Assisted Jet Electrochemical Machining. Proceedings of the EUSPEN 10th Anniversary International Conference 2:420–424.
[5] Kai S, Kunieda M (2013) Study on Effect of Assist Gas in Electrolyte Jet Machining. Denki Kako Gakkaishi 47(115):97–103. in Japanese.
[6] Bisterov I, Abayzeed S, Speidel A, Magnini M, Zubayr M, Clare AT (2023) Adapting 'Tool' Size Using Flow Focusing: A New Technique for Electrochemical Jet Machining. *Journal of Materials Processing Technology* 311:117807.
[7] Li X, Ming P, Zhang X, Wang W, Zhang Y, Qin G, Zheng X, Niu S (2020) Compressed Air-Film Encircling Jet Electrodeposition with High Deposition Accuracy. *Journal of The Electrochemical Society* 167(10):102502.
[8] Liu G, Tong H, Shi H, Li Y, Li J (2022) Fabrication of a Tool Electrode with Hydrophobic Features and its Stray-Corrosion Suppression Performance for Micro-Electrochemical Machining. *Langmuir* 38(8):2711–2719.
[9] Wüthrich R, Hof LA (2006) The Gas Film in Spark Assisted Chemical Engraving (SACE) - A Key Element for Micro-Machining Applications. *International Journal of Machine Tools and Manufacture* 46(7–8):828–835.
[10] Zhan S, Liu B, Yu X, Chen X, Zeng G, Zhao Y (2023) Fabrication of Homogeneous Nanoporous Structure on 4H-/6H-SiC Wafer Surface via Efficient and Eco-Friendly Electrolytic Plasma-Assisted Chemical Etching. *Small* 19(14):2205720.
[11] Zhan S, Lyu Z, Dong B, Liu W, Zhao Y (2023) Cathodic Discharge Plasma in Electrochemical Jet Machining: Phenomena, Mechanism and Characteristics. *International Journal of Machine Tools and Manufacture* 187:104015.
[12] Yerokhin AL, Nie X, Leyland A, Matthews A, Dowey SJ (1999) Plasma Electrolysis for Surface Engineering. *Surface and Coatings Technology* 122(2–3):73–93.
[13] Gupta P, Tenhundfeld G, Daigle EO, Ryabkov D (2007) Electrolytic Plasma Technology: Science and Engineering—An Overview. *Surface and Coatings Technology* 201(21):8746–8760.
[14] Gupta SKS, Singh R (2016) Cathodic Contact Glow Discharge Electrolysis: Its Origin and Non-Faradaic Chemical Effects. *Plasma Sources Science and Technology* 26 (1):015005.